Available online at www.sciencedirect.com

SciVerse ScienceDirect

Ceramics International 39 (2013) 111–119

CERAMICS INTERNATIONAL

www.elsevier.com/locate/ceramint

Sintering properties of hydroxyapatite powders prepared using different methods

S. Ramesh[a,*], K.L. Aw[b], R. Tolouei[c], M. Amiriyan[c], C.Y. Tan[b], M. Hamdi[a], J. Purbolaksono[a], M.A. Hassan[a], W.D. Teng[d]

[a]*Department of Engineering Design and Manufacturing, Advanced Manufacturing and Material Processing (AMMP) Centre, University of Malaya, 50603 Kuala Lumpur, Malaysia*

[b]*Ceramics Technology Laboratory, 43009 Kajang, Selangor, Malaysia*

[c]*Faculty of Science and Engineering, Laval University, Quebec, Canada G1V 0A6*

[d]*Ceramics Technology Group, SIRIM Berhad, 1 Persiaran Dato Menteri, Shah Alam, Malaysia*

Received 10 May 2012; received in revised form 31 May 2012; accepted 31 May 2012
Available online 15 June 2012

Abstract

In the present work, the sintering behaviour of HA particles prepared via the wet precipitation method (HAp) and wet mechanochemical technique (HAwm) was investigated. The sintering behaviour of a commercial HA powder (HAc) was also studied for comparison purpose. All the three powders were characterised in terms of particle size, Ca/P ratio and crystal size. Green samples were prepared and sintered in air at temperatures ranging from 1000 °C to 1400 °C. The sintered bodies were studied in terms of the phase stability, relative density, Young's modulus, Vickers hardness, fracture toughness and grain size. The results indicated that HAwm samples suffered phase decomposition while the HAp and HAc sintered samples showed no phase disruption throughout the temperature range employed. The HAp samples exhibited the overall best densification and properties when compared to the HAc and HAwm samples. Furthermore, the results showed that mechanical properties of sintered samples were governed by both the bulk density and the grain size.

Keywords: C. Mechanical properties; Hydroxyapatite; Sinterability; Synthesis

1. Introduction

The bones in human body are known to possess a unique ability to regenerate and remodel without leaving a scar [1]. Apart from that, it also provides mechanical stability needed for support, locomotion and protection of vital organs [2,3]. Even though bones have unique abilities, it is known to be susceptible to fracture and degenerative diseases [4]. When bones are lost and required restoration, it can be done through transplantation or implantation [5]. The transplantation method involves the harvesting of bone tissues from a donor which would be transplanted into the host site [6]. However, the use of this method is complicated due to considerations such as cost, defect's size, availability of grafts, potentially damaging of donor tissues including the tendency of viral and bacterial infections [7,8]. On the other hand, the implantation method involved the use of synthetic materials that are easily available, reproducible and reliable [5,9].

Amongst the synthetic materials considered for biomedical applications, hydroxyapatite (HA) bioceramic having a chemical formula of $Ca_{10}(PO_4)_6(OH)_2$ correlates well with the mineral component of human hard tissues [10]. Moreover, HA exhibits excellent stability in aqueous medium with pH above 4.3, well within the range of blood which has a pH of about 7.3 [4,11]. Furthermore, due to the similarity in chemical structure to human hard tissues, HA tends to exhibit properties such as bioactivity and biocompatibility [12,13]. However, researchers found that to use HA effectively in medical applications, the powders must have a well-defined particle morphology [14,15].

*Corresponding author. Tel.: +603 7967 5382; fax: +603 7967 5330.
E-mail address: ramesh79@um.edu.my (S. Ramesh).

0272-8842/$36.00
http://dx.doi.org/10.1016/j.ceramint.2012.05.103

Therefore, researchers studied and developed various synthesis method such as wet chemical method [16,17], mechanochemical method [18], sol–gel method [19,20] and the hydrothermal method [21–23].

Besides the powder processing methods, the other most important controlling parameter that has a profound effect on the properties of hydroxyapatite is the powder consolidation/sintering method. The most commonly used method of powder consolidation is the conventional pressureless sintering method. This technique often requires long sintering schedule, typically above 18 h which could result in grain coarsening. A more rapid, yet effective technique would be the microwave sintering which has been reported to produce a dense sintered HA body that possessed fine microstructure coupled with improved mechanical properties [23–28].

The primary objective of this research is to study the sinterability of HA powders prepared through wet chemical method and wet mechanochemical method. In addition, the sintering behaviour of a commercial HA powder was also studied for comparison purpose.

2. Methods and materials

In the present work, one batch of HA powder was prepared through a wet chemical method comprising precipitation from aqueous medium by addition of orthophosphoric acid to calcium hydroxide solution, with the pH maintained above 10 [29]. Once the titration process completed, the suspension was allowed to age overnight. Then, the precipitate was filtered, washed, dried and ground to a fine powder hereafter known as "HAp". Another batch of HA powder, hereafter known as "HAwm", was prepared according to the wet mechanochemical method proposed by Rhee [30]. The starting precursors used were commercially available calcium pyrophosphate, $Ca_2P_2O_7$ (99.9% purity, Aldrich) and calcium carbonate, $CaCO_3$ (99% purity, Aldrich). In order to evaluate the sinterability and performance of the synthesised HA, a commercial HA powder manufactured by Merck, Germany was also studied, hereafter known as "HAc". Disc and bar samples were prepared through uniaxial pressing at 1.3–2.5 MPa followed by cold isostatic pressing at 200 MPa (Reiken Seiki, Japan). The resulting green samples were consolidated by pressureless sintering in air over the temperature range of 1000 °C–1400 °C, using a ramp rate of 2 °C/min (heating and cooling) and soaking time of 2 h for each firing. All sintered samples were polished to a 1 μm finish prior to testing.

The Ca/P ratio of the powders was analysed through the Inductively Coupled Plasma-Atomic Emission Spectrometry (ICP-AES) technique while the powder particle size was obtained using a standard Micromeritics® SediGraph 5100 X-ray particle analyser. Phase analysis of the synthesised powders and sintered samples were done by using X-ray diffraction (XRD) (Rigaku Geiger-Flex, Japan) under ambient conditions using Cu-Kα as the radiation source at a scan speed of 3°/min and a step scan of 0.02°. The peaks obtained were compared to standard reference JCPDS files. The phase stability of the HA powders was further confirmed through the use of Fourier transfer infrared (FTIR—Brukers IFS-66-VS) testing. The bulk densities of the samples were measured by Archimedes' method, using distilled water as the immersion media and the relative density was calculated by taking the theoretical density of HA as 3.156 gcm^{-3}. The Young's modulus (E) was determined by sonic resonance method for rectangular samples using a commercial testing instrument (Grindo-Sonic: MK5 "Industrial", Belgium) [31].

Both the hardness (H_V) and fracture toughness (K_{Ic}) values were obtained from the Vickers microhardness test (Matsuzawa, Japan) [32]. The applied load used for each indentation was set at 50 g with a dwell time of 10 s. Three indentations were made for each sample and the average value was taken. Apart from that, the morphology of the powder and the microstructure development of the sintered samples were examined through scanning electron microscope (SEM, Philips XL130). The grain size of sintered HA was determined from the SEM micrographs using the line intercept method [33].

3. Results and discussion

The XRD profiles of HA powders shown in Fig. 1 revealed that there was no phase decomposition of HA into secondary phases such as α-TCP, β-TCP, TTCP or CaO. However, there is a significant difference in terms of the degree of crystallinity between the HAp, HAwm and HAc powders as observed from the peak broadening. The HAp and HAc powders exhibited broader peaks (Fig. 1b and c) which signify that the powders have low crystallinity. This is very typical of a HA powder prepared via the wet chemical route [34,35].

In contrast, the XRD peak of HAwm powder revealed significantly different characteristics of sharper and narrow diffraction peaks which indicate that the material is highly

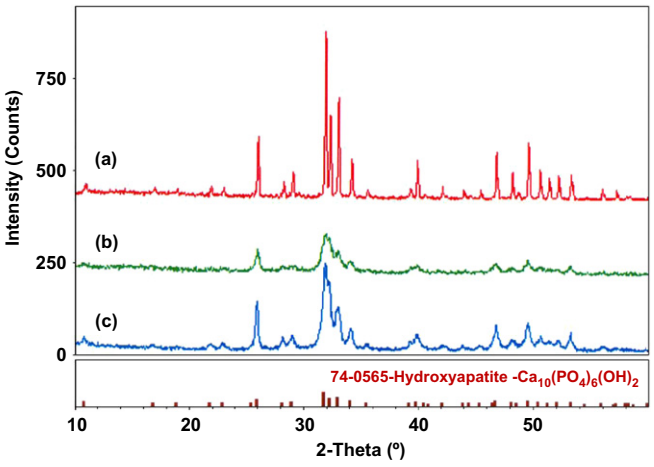

Fig. 1. As-received XRD patterns of HA powders (a) HAwm, (b) HAp and (c) HAc.

crystalline. This can be associated with the heat treatment process employed as part of the mechanochemical treatment [36,37]. Nonetheless, the XRD signatures of all three powders conform to the stoichiometric HA profile as depicted in Fig. 1.

The FTIR analysis of all three HA powders is given in Fig. 2. The results showed that all the HA powders exhibited FTIR spectrum that corresponded to stoichiometric HA. Moreover, it was observed that all the HA powders spectrum revealed bands belonging to PO_4^{3-} group at 470 cm^{-1}, 560–610 cm^{-1}, 960 cm^{-1} and 1000–1100 cm^{-1} [38–40] including the characteristics bands due to apatitic OH^- in the HA matrix at 3570 cm^{-1} (stretching) and 630 cm^{-1} (liberation/bending) [8,41,42].

However, the spectrum for HAp also exhibited prominent broad peaks around 3400 cm^{-1} (stretching) and 1650 cm^{-1} (bending). These peaks are assigned to chemically absorbed H_2O and corresponds to the characteristic of HA prepared by an aqueous precipitation route [43,44]. A similar observation was made for the FTIR spectrum of the commercial HAc powder and this is in agreement with the work of other researchers [45,46].

On the contrary, the FTIR spectrum of HAwm synthesised through mechanochemical process showed that the peaks around 3400 cm^{-1} (stretching) and 1650 cm^{-1} (bending) were not present. However, the characteristics bands due to apatitic OH^- in the HA matrix were present at 3570 cm^{-1} (stretching) and 630 cm^{-1} (libration) despite undergoing the heat treatment at 1100 °C. It is believed that the basic apatitic structure of HAwm powder was not affected by the heat treatment except that the chemically absorbed water during powder processing disappeared after the heat treatment at 1100 °C. Similar FTIR observations were reported in the literatures for heat-treated HA powders [42–44].

The chemical analysis of all the HA powder yielded results as shown in Table 1. The results showed that all three HA powders have a Ca/P ratio within the stoichiometric range of 1.67. This is important because deviation from stoichiometric value would affect the HA phase stability, reactivity, degradability, densification and mechanical properties of the sintered body [47–51].

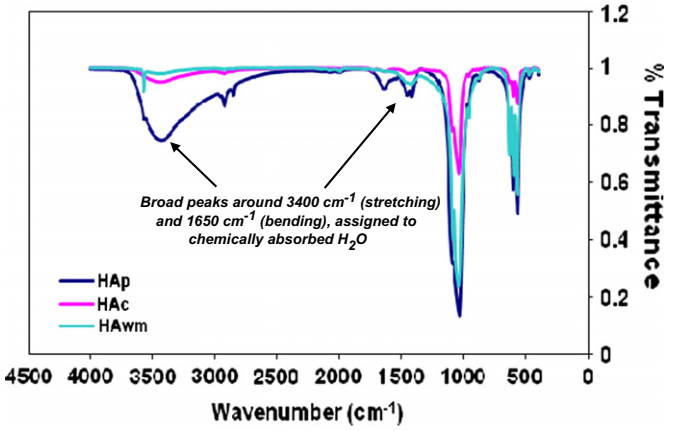

Fig. 2. FTIR spectrums of the HA powders.

Table 1
Properties of HA starting powder.

	(HAp)	(HAwm)	(HAc)
Crystallite size (nm)	108	> 1000	151
Degree of crystallinity (%)	27	91	30
Specific surface area (m^2/g)	60.74	2.68	60.16
Calcium (%w/w)	38.90	38.48	37.00
Phosphorus (%w/w)	23.20	23.03	22.00
Ca/P ratio	1.67 ± 0.01	1.67 ± 0.01	1.67 ± 0.02

The estimation of crystal size from peak broadening was based on Scherrer's formula [46,52–54] for the HA powders studied taken at the (2 1 1) peak as shown in Table 1. The results showed that the HAp powder has crystals size smaller than the HAc crystals and lies within the nanometre range. In contrast, the HAwm powder prepared through wet mechanochemical method has very large crystals size in the submicron range due to the heat treatment of the powder. Additionally, it has been reported that small crystals' size are favourable due to the ability of exhibiting much higher bioactivity when compared to coarse crystals. Moreover, the finer crystals also provided larger interfaces for osseointegration [8,17,22,55–58].

The SEM images of HA powders were in agreement with the crystallite size estimations. As shown in Fig. 3, the synthesised HAp consists of a mixture of fine powders having particles ranging from 1–3 μm in diameter. On the other hand, the particle size of the wet mechanochemical method powder was in the range of 2–5 μm in diameters, though the powder consisted of hard agglomerates as shown in Fig. 3c. This observation is in agreement with that reported by Kumta et al. [59] for heat treated HA powders. The commercial HAc powder was observed to consist of larger particles, up to 10 μm, as typically shown in Fig. 3b.

The XRD traces of the HAp and HAc samples exhibited phase that corresponds to stoichiometric HA with no secondary phases being detected as shown in Figs. 4 and 5. As for the HAwm sintered samples, the XRD traces showed that decomposition into TTCP occurred when sintering was carried out above 1250 °C as shown in Fig. 6. The emergence of tetra-calcium phosphate (TTCP) was probably due to the effect of calcination carried out on the HAwm powder which could have caused the dehydroxylation of HA to complete during sintering [55,60,61]. Some researchers have reported that decomposition into secondary phases proceeded above 1350 °C [45] while some reported that decomposition occurred when sintered at 1200 °C [55,62].

The effect of sintering on the bulk density of HA is shown in Fig. 7. The results indicated that the HAp samples exhibited better densification for temperature of 1000 °C–1400 °C when compared to that exhibited by the

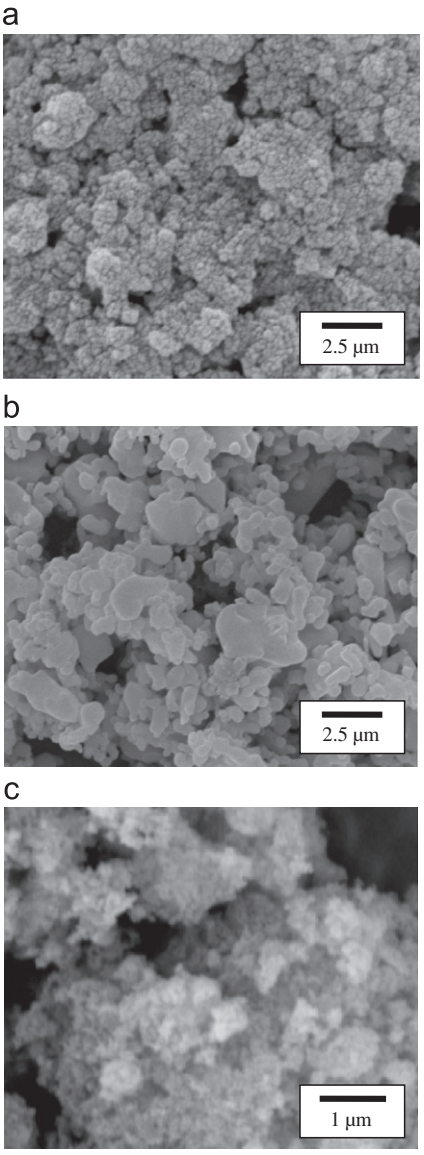

Fig. 3. SEM micrographs of (a) Hap powder revealing the presences of loosely packed particles, (b) HAwm revealing, neck formation between particles, and presences of hard particles and (c) HAc powder revealing larger and more compacted agglomerates.

HAc and HAwm samples for the same temperature range. Moreover, it can be observed that the onset of sintering for HAp is between 900 and 1000 °C i.e. 200 °C lower than for both the HAc and HAwm which occurred between 1100 and 1200 °C.

The HAp samples had a relative density of ~93% at 1000 °C and attained a final density of ~98% when sintered above 1050 °C. At a similar temperature of 1000 °C, the HAc and HAwm samples attained only ~67% and ~65% of theoretical density, respectively. Moreover, for the HAc to achieve final densification of ~98% of theoretical density requires the samples to be sintered at 1250 °C. This was in agreement with the findings of Georgiou et al. [63] for commercially available

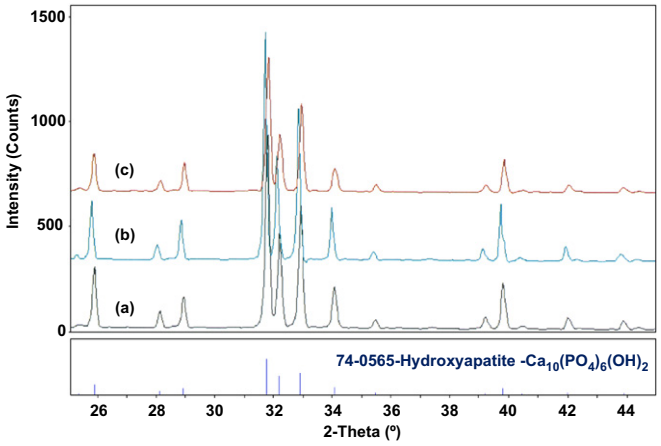

Fig. 4. XRD traces of HAp sintered samples (a) 1000 °C, (b) 1200 °C and (c) 1400 °C.

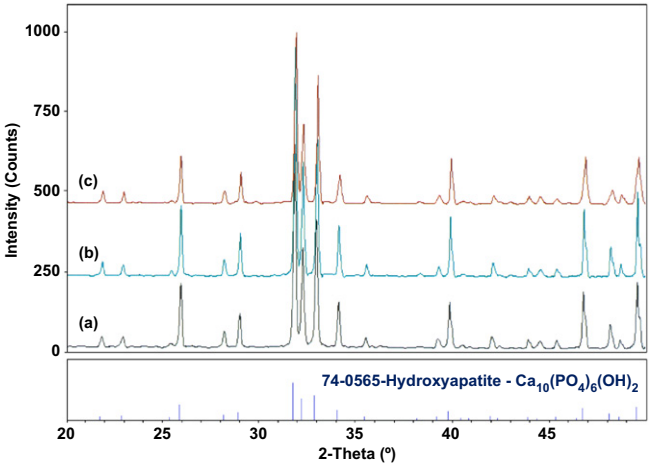

Fig. 5. The XRD traces of HAc samples sintered at (a) 1000 °C, (b) 1200 °C and (c) 400 °C.

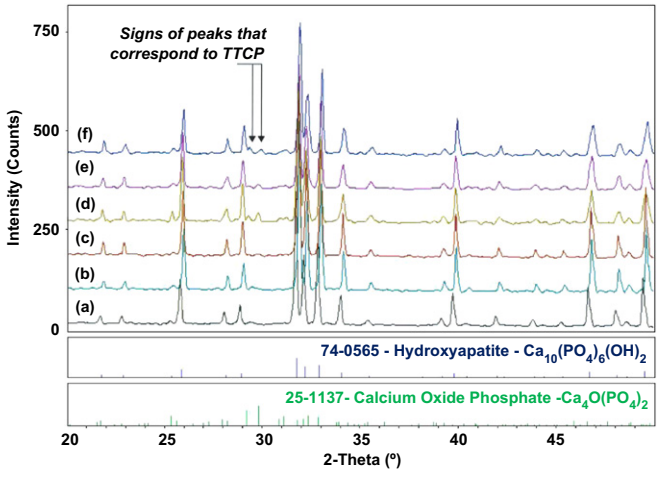

Fig. 6. The XRD traces of synthesised HAwm sintered at (a) 1000 °C, (b) 1200 °C, (c) 1250 °C, (d) 1300 °C, (e) 1350 °C and (f) 1400 °C.

powder. In contrast, the HAwm samples exhibited ~95% density when sintered at 1350 °C and achieved a maximum of ~96% relative density when sintered at 1400 °C.

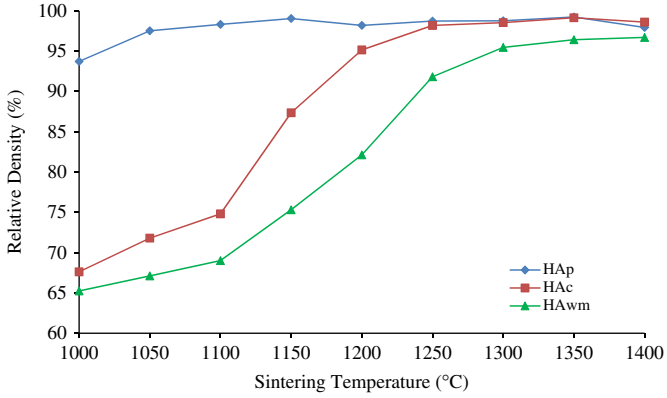

Fig. 7. The effect of sintering temperature on the relative density of sintered HA.

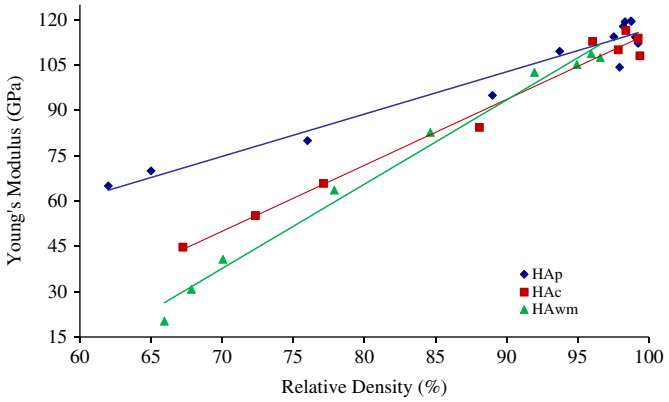

Fig. 9. A linear relationships exists between the sintered density and Young's modulus of hydroxyapatite ceramics.

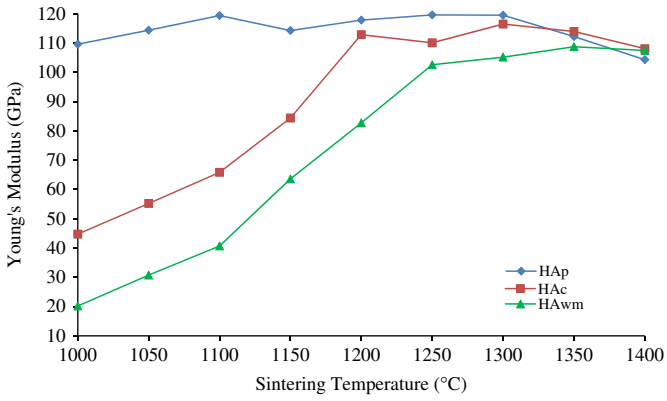

Fig. 8. Young's modulus variation with sintering temperature of hydroxyapatite samples.

The HAp sample showed better densification than either HAc or HAwm probably due to the finer particle size which in turn increases the heat transfer area of the particles during sintering [62,64–66]. On the contrary, the HAwm comprising of hard agglomerates as seen in Fig. 3c could have led to a lower packing density in the green state and resulting in poor densification [67,68].

The effects of sintering temperature on Young's modulus (E) of the HA is shown in Fig. 8. Both Young's modulus of HAc and HAwm samples was found to increase with increasing temperature. It was observed that at sintering temperature of 1000 °C, Young's modulus attained by the HAc and HAwm samples was about 50 GPa and 20 GPa, respectively. As the sintering temperature was increased, the E of both HAc and HAwm samples increased almost linearly, achieving ~100 GPa at 1200 °C and 1250 °C, respectively. Young's modulus of HAc samples peaked at 116 GPa when sintered at 1300 °C while the HAwm samples peaked at ~108 GPa when sintered at 1350 °C. On the contrary, HAp samples attained a high E value of ~110 GPa when sintered at low temperature of 1000 °C and did not change very much with further increase in temperature. In addition, attempts to correlate Young's modulus and bulk density revealed a linear trend existed between both properties as shown in Fig. 9. This observation is in agreement with the work of He et al. [9] who reported that Young's modulus of HA is controlled by the pore volume fraction in the sintered body.

The SEM images of samples fired at 1200 °C showed that commercial HAc and mechanochemical HAwm have high amount of pores, see Fig. 10. In contrast, the HAp samples (Fig. 10b) showed a dense microstructure. In addition, a uniform grain size was observed for the HAc and HAwm samples sintered at 1200 °C and this is in agreement with that reported by Muralithran and Ramesh [45]. On the other hand, the HAp samples exhibited a bimodal distribution of grains, with the presences of some individual large grains, ranging between 1 and 3 μm in diameter as shown in Fig. 10b. This was more pronounce for samples sintered at 1350 °C with some grains grew up to 10–12 μm (Fig. 10e). The average grain variation with sintering temperature is shown in Fig. 11. All three HA samples exhibited increasing grain size trend with increasing sintering temperature with the HAp samples exhibited a higher rate of grain growth. This trend of grain size increased with sintering temperature was also found for HA sintered using rapid sintering method such as in microwave. For instance, Fang et al. [26] found that the grain size of the microwave sintered HA increased with sintering temperature and holding time but at a much slower rate when compared to that sintered via the conventional sintering method. Typically for the same sintering temperature of 1300 °C, the grain size of both microwave and conventionally sintered samples increased substantially, but was at a much slower rate in the microwave sintered HA i.e. the grain size of the microwave sintered sample increased from 2.06 μm (5 min holding time) to 3.30 μm (20 min holding time) whereas the conventional sintered sample exhibited a grain size of 6.52 μm. Similar grain size trend was also reported by other researchers [28,42]. In addition, Fang et al. [26] found that the occurrence of abnormal grain growth was more pronounced in the conventionally sintered samples and this is in good agreement with the microstructural observation in the present HA.

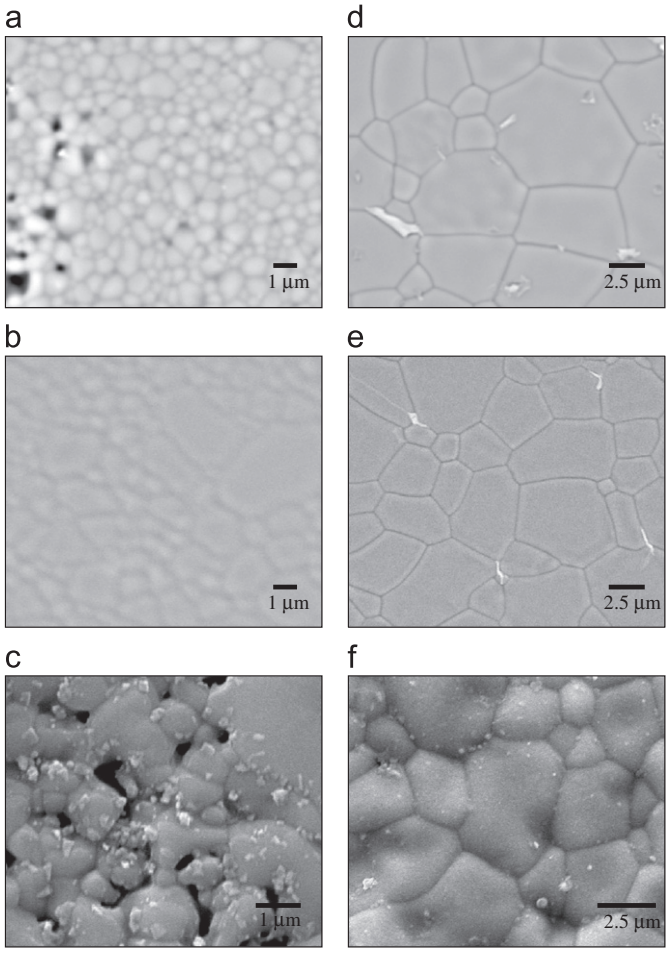

Fig. 10. Images of HAc sintered at (a) 1200 °C, (d) 1350 °C, HAp sintered at (b) 1200 °C, (e) 1350 °C, and HAwm (c) 1200 °C and (f) 1350 °C.

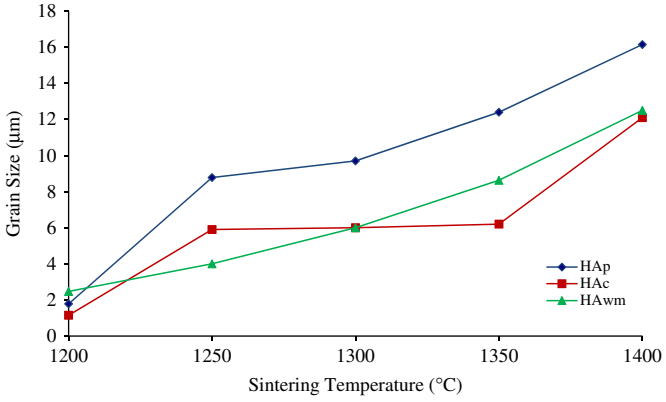

Fig. 11. Average grain size variation with sintering temperature for HA sintered at various temperatures.

The effect of sintering temperature on the Vickers hardness of HA is shown in Fig. 12. It was observed that the sintered HAp samples exhibited superior hardness when compared to HAc and HAwm sintered samples. Furthermore, the HAp samples were generally seen to attain hardness of ~5 GPa across the sintering range with

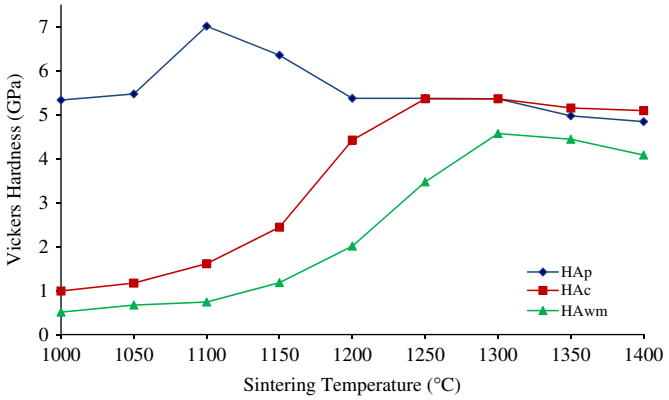

Fig. 12. Effect of sintering temperature on the Vickers hardness of hydroxyapatite.

a maximum of ~7.01 GPa achieved when sintered at 1100 °C. On the other hand, the HAc and HAwm samples exhibited an increasing hardness trend with increase temperature, i.e. the hardness was about 1 GPa and 0.51 GPa at 1000 °C and increased to a maximum of about 5.36 GPa and 4.57 GPa at 1300 °C, respectively. The hardness values were found to decrease when sintered above 1300 °C for both the HAc and HAwm samples as shown in Fig. 12 due to grain coarsening. This result is not in agreement with the findings of Curran et al. [69] who reported that the hardness of their microwave sintered HA increased with increasing grain size. In addition, these authors found that the hardness of both conventional sintered and microwave sintered samples was dependent on the on the level of open (surface) porosity. These differences in hardness result obtained between the present work with that reported in the literatures could be associated to the different powder characteristics resulting from different synthesis method employed to prepare the hydroxyapatite powder.

In agreement with the hardness trend, the fracture toughness, K_{Ic} of HAp sintered samples was observed to attain superior value throughout the sintering range when compared to both HAc and HAwm samples as shown in Fig. 13. The HAp samples attained an average K_{Ic} of about 0.7 $MPam^{1/2}$ across the sintering range with maximum of 0.9 $MPam^{1/2}$ achieved at 1050 °C. On the other hand, the value of K_{Ic} for HAc and HAwm samples were only measurable starting from temperature of 1100 °C and 1200 °C, respectively. The commercial HAc sintered samples showed an increasing trend of fracture toughness from 0.35 $MPam^{1/2}$ at 1100 °C and reached a maximum of 0.76 $MPam^{1/2}$ at 1300 °C before decreasing with further increase in the sintering temperature. Similarly, the K_{Ic} of HAwm increases with sintering temperature from 0.53 $MPam^{1/2}$ at 1200 °C and peaked at ~0.7 $MPam^{1/2}$ for sintering temperature of 1300 °C before decreasing with further sintering.

The decreased in K_{Ic} observed by all the HA samples after reaching a maximum value could be associated with

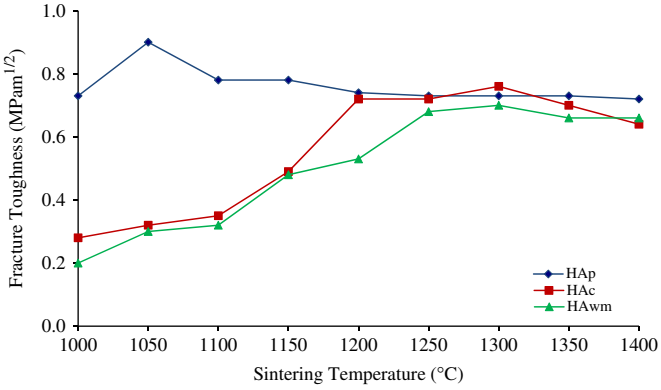

Fig. 13. Effect of sintering temperature on the fracture toughness of HA.

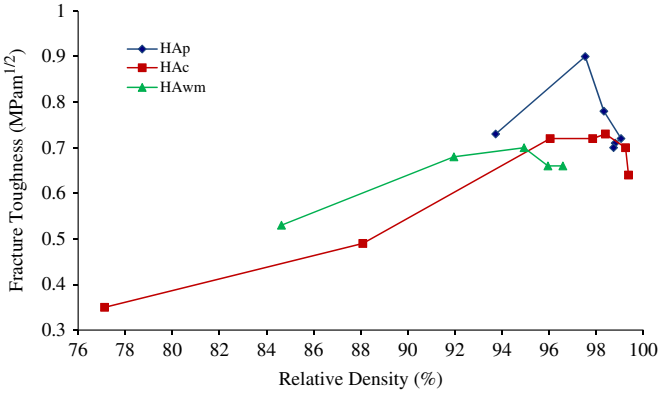

Fig. 14. Fracture toughness variations with relative density for HAp, HAc and HAwm samples.

grain growth [70–75]. For instance, Bose et al. [42] reported a high fracture toughness of 1.9 ± 0.2 MPam$^{1/2}$ which was obtained for microwave sintered sample having a grain size of 168 ± 86 nm when compared to 1.2 ± 0.2 MPam$^{1/2}$ for 1.16 ± 0.17 μm grain size. The present study found that the fracture toughness of HA was dependent on the bulk density as depicted in Fig. 14. The results showed that the fracture toughness increased with increasing relative density up to 95% for HAwm samples, 97.5% for HAp samples and 98% for HAc samples before decreasing with further increase in relative density. This decrease in the fracture toughness as observed for the three set of samples could be associated with HA grain coarsening. This can be seen from Fig. 15 which revealed that the HA grain continue to grow with little or no further increase in the relative density. These results suggested that at low temperatures below 1250 °C, the fracture toughness is governed by bulk density. However, when the grain size increased to beyond a certain limit, i.e. about 6 μm for HAwm, about 6.5 μm for HAc and about 8.8 μm for HAp, the toughness would decrease even though the bulk density remained above 95% of the theoretical value.

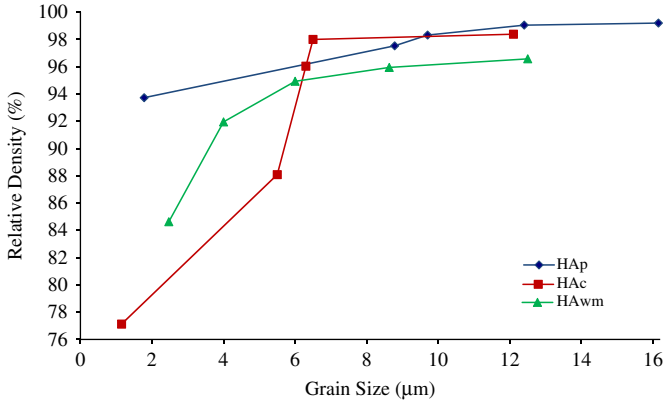

Fig. 15. Relative density variation with grain size for HA samples.

4. Conclusions

The present work reports on the sintering behaviour of HA powder produced by two different routes. It was found that HA powder synthesised through the wet mechanochemical method tend to produce powders that consisted of hard agglomerates while the wet chemical method powder consisted of soft agglomerates comprising of loosely packed particles. It was shown that the HAp compacts exhibited superior sinterability properties especially at low sintering temperature between 1000 °C and 1200 °C. In comparison, HAc and HAwm powders required sintering to be carried out at 1200 °C and above to achieve similar results. The sintered HAp and HAc samples were found to exhibit XRD signatures that correspond to stoichiometric HA. In contrast, the HAwm sintered samples showed traces of TTCP in the structure when sintering was carried out at 1300 °C and above.

In terms of mechanical properties, the HAp samples exhibited matrix stiffness of above ~100 GPa while the HAc and HAwm samples only managed to produce similar result at 1200 °C and 1250 °C, respectively. It was also revealed that Young's modulus of HA varied linearly with bulk density. The synthesised HAp samples were also found to have superior hardness and fracture toughness in comparison to the commercial HAc and wet mechanochemically synthesised HAwm samples. The study also found that the fracture toughness could be related to both, relative density and grain growth of the sintered samples.

Acknowledgement

This study was supported under the HIR Grant no. H-16001-00-D000027. The authors gratefully acknowledge the Ministry of Higher Education Malaysia for the financial support.

References

[1] U. Kneser, D.J. Schaefer, E. Polykandriotis, R.E. Horch, Tissue engineering of bone: the reconstructive surgeon's point of view, Journal of Cellular and Molecular Medicine 10 (2006) 7–19.

[2] J.E. Davies, Bone bonding at natural and biomedical surfaces, Biomaterials 28 (2007) 5058–5067.
[3] V.I. Sikavitsas, J.S. Temenoff, A.G. Mikos, Biomaterials and bone mechanotransduction, Biomaterials 22 (2001) 2581–2593.
[4] S.M. Best, A.E. Porter, E.S. Thian, J. Huang, Bioceramics: past, present and for the future, Journal of the European Ceramic Society 28 (2008) 1319–1327.
[5] L.L. Hench, The challenge of orthopaedic materials, Current Orthopaedics 14 (2000) 7–15.
[6] P.V. Giannoudis, H. Dinopoulus, E. Tsiridis, Bone substitutes: an update, Injury—International Journal of the Care of the Injured 365 (2005) 520–527.
[7] T. Kokubo, H.M. Kim, M. Kawashita, Novel bioactive materials with different mechanical properties, Biomaterials 24 (2003) 2161–2175.
[8] R. Murugan, S. Ramakrishna, Aqueous mediated synthesis of bioresorbable nanocrystalline hydroxyapatite, Journal of Crystal Growth 274 (2005) 209–213.
[9] L.H. He, O.C. Standard, T.T.Y. Huang, B.A. Latella, M.V. Swain, Mechanical behaviour of porous hydroxyapatite, Acta Biomaterialia 4 (2008) 577–586.
[10] Y. Liu, D. Hou, G. Wang, A simple wet chemical synthesis and characterization of hydroxyapatite nanorods, Materials Chemistry and Physics 86 (2004) 69–73.
[11] S.J. Kalita, S. Bose, H.L. Hosick, A. Bandyopadhyay, $CaO–P_2O_5–Na_2O$-based sintering additives for hydroxyapatite (Hap) ceramics, Biomaterials 25 (2004) 2331–2339.
[12] A.R. Calafiori, G. Di Marco, G. Martino, M. Marotta, Preparation and characterization of calcium phosphate biomaterials, Journal of Materials Science: Materials in Medicine 18 (2007) 2331–2338.
[13] B. Cengiz, Y. Gokce, N. Yildiz, Z. Aktas, A. Calimli, Synthesis and characterization of hydroxyapatite nanoparticles, Colloids and Surfaces A: Physicochemical and Engineering Aspects 322 (2008) 29–33.
[14] N.Y. Mostafa, Characterization, thermal stability and sintering of hydroxyapatite powders prepared by different routes, Materials Chemistry and Physics 94 (2005) 333–341.
[15] L.M. Rodriguez-Lorenzo, M. Vallet-Regi, J.M.F. Ferreira, Fabrication of hydroxyapatite bodies by uniaxial pressing from a precipitated powder, Biomaterials 22 (2001) 583–588.
[16] A. Afshar, M. Ghorbani, N. Ehsani, M.R. Saeri, C.C. Sorrell, Some important factors in the wet precipitation process of hydroxyapatite, Materials and Design 24 (2003) 197–202.
[17] I. Mobasherpour, M.S. Heshajin, A. Kazemzadeh, M. Zakeri, Synthesis of nanocrystalline hydroxyaptite by using precipitation method, Journal of Alloys and Compounds 430 (2007) 330–333.
[18] G. Bezzi, G. Celotti, E. Landi, T.M.G. La Torretta, I. Sopyan, A. Tampieri, A novel sol–gel technique for hydroxyapatite preparation, Materials Chemistry and Physics 78 (2003) 816–824.
[19] W. Weng, G. Han, P. Du, G. Shen, The effect of citric acid addition on the formation of sol–gel derived hydroxyapatite, Materials Chemistry and Physics 74 (2002) 92–97.
[20] J. Liu, X. Ye, H. Wang, M. Zhu, B. Wang, H. Yan, The influence of pH and temperature on the morphology of hydroxyapatite synthesized by hydrothermal method, Ceramics International 121 (2002) 59–64.
[21] I.R. Gibson, S. Ke, S.M. Best, W. Bonfield, Effect of powder characteristics on the sinterability of hydroxyapatite powders, Journal of Materials Science: Materials in Medicine 12 (2001) 163–171.
[22] M.H. Santos, M. de Oliveira, L.P. de Freitas Souza, H.S. Mansur, W.L. Vasconcelos, Synthesis control and characterization of hydroxyapatite prepared by wet precipitation process, Materials Research 7 (2004) 625–630.
[23] Y. Fang, D.K. Agrawal, D.M. Roy, R. Roy, Fabrication of transparent hydroxyapatite ceramics by microwave processing, Materials Letters 23 (1995) 147–151.
[24] Y. Fang, D.K. Agrawal, D.M. Roy, R. Roy, Rapid sintering of hydroxyapatite by microwave processing, in: D.E. Clark, F.D. Gac, W.H. Sutton (Eds.), Ceramic Transactions, Microwaves: Theory and Applications in Material Processing, vol. 21, Am. Ceram. Soc. Publ., Westerville, OH, 1991, pp. 349–356.
[25] D.K. Agrawal, Y. Fang, D.M. Roy, R. Roy, Fabrication of hydroxyapatite ceramics by microwave processing, in: R.L. Beatty, W.H. Sutton, M.F. Iskander (Eds.), Materials Research Society Symposium, Microwave Processing of Materials III, vol. 269, MRS publ., Pittsburgh, 1992, pp. 231–236.
[26] Y. Fang, D.K. Agrawal, D.M. Roy, R. Roy, Microwave sintering of hydroxyapatite, Journal of Materials Research 9 (1994) 180–187.
[27] A. Chanda, S. Dasgupta, S. Bose, A. Bandyopadhyay, Microwave sintering of calcium phosphate ceramics, Materials Science and Engineering C 29 (2009) 1144–1149.
[28] S. Ramesh, C.Y. Tan, S.B. Bhaduri, W.D. Teng, Rapid densification of nanocrystalline hydroxyapatite for biomedical application, Ceramics International 33 (2007) 1363–1367.
[29] S. Ramesh, A Method for Manufacturing Hydroxyapatite Bioceramic, Malaysia Patent no. PI. 20043325, 2004.
[30] S.H. Rhee, Synthesis of hydroxyapatite via mechanochemical treatment, Biomaterials 23 (2002) 1147–1152.
[31] ASTM Standard C1259—2008e1, Standard Test Method for Dynamic Young's Modulus, Shear Modulus, and Poisson's Ratio for Advanced Ceramics by Impulse Excitation of Vibration, ASTM International, West Conshohocken, PA, 2008.
[32] ASTM C1327-08, Standard Test Method for Vickers Indentation Hardness of Advanced Ceramics, ASTM International, West Conshohocken, PA, 2008.
[33] ASTM E112-96(2004)e2, Standard Test Methods for Determining Average Grain Size, ASTM International, West Conshohocken, PA, 2004.
[34] Y.X. Pang, X. Bao, Influence of temperature, ripening time and calcinations on the morphology and crystallinity of hydroxyapatite nanoparticles, Journal of the European Ceramic Society 23 (2003) 1697–1704.
[35] J. Wang, L. Shaw, Transparent nanocrystalline hydroxyapatite by pressure-assisted sintering, Scripta Materialia 63 (2010) 593–596.
[36] H.Y. Juang, M.H. Hon, Effect of calcinations in the sintering of hydroxyapatite, Biomaterials 17 (1996) 2059–2064.
[37] S. Kim, Y.M. Kong, I.S. Lee, H.E. Kim, Effect of calcinations of starting powder on mechanical properties of hydroxyapatite-alumina bioceramics composite, Journal of Materials Science: Materials in Medicine 13 (2002) 307–310.
[38] A. Antonakos, E. Liarokapis, T. Leventouri, Micro-Raman and FTIR studies of synthetic and natural apatites, Biomaterials 28 (2007) 3043–3054.
[39] A. Bianco, I. Cacciotti, M. Lombardi, L. Montanaro, G. Gusmano, Thermal stability and sintering behaviour of hydroxyapatite nanopowders, Journal of Thermal Analysis and Calorimetry 88 (2007) 237–243.
[40] S. Pramanik, A.K. Agarwal, K.N. Rai, A. Garg, Development of high strength hydroxyapatite by solid-state sintering process, Ceramics International 33 (2007) 419–426.
[41] C.W. Chen, C.S. Oakes, K. Byrappa, R.E. Riman, K. Brown, K.S. TenHuisen, V.F. Janas, Synthesis, characterization, and dispersion properties of hydroxyapatite prepared by mechanochemical–hydrothermal methods, Journal of Materials Chemistry 14 (2004) 2425–2432.
[42] S. Bose, S. Dasgupta, S. Tarafder, A. Bandyopadhyay, Microwave-processed nanocrystalline hydroxyapatite: simultaneous enhancement of mechanical and biological properties, Acta Biomaterialia 6 (2010) 3782–3790.
[43] H. Nishikawa, Thermal behavior of hydroxyapatite in structural and spectrophotometric characteristics, Materials Letters 50 (2001) 364–370.
[44] D. Choi, P.N. Kumta, An alternative chemical route for the synthesis and thermal stability of chemically enriched hydroxyapatite, Journal of the American Ceramic Society 88 (2006) 444–449.
[45] G. Muralithran, S. Ramesh, The effects of sintering temperature on the properties of hydroxyapatite, Ceramics International 26 (2000) 221–230.

[46] C.C. Silva, A.G. Pinheiro, M.A.R. Miranda, J.C. Goes, A.S.B. Sombra, Structural properties of hydroxyapatite obtained by mechanosynthesis, Solid State Sciences 5 (2003) 553–558.
[47] S. Raynaud, E. Champion, D. Bernache-Assollant, P. Thoma, Calcium phosphate apatites with variable Ca/P atomic ratio I. Synthesis, characterisation and thermal stability of powders, Biomaterials 23 (2002) 1065–1072.
[48] S. Raynaud, E. Champion, D. Bernache-Assollant, Calcium phosphate apatites with variable Ca/P atomic ratio II. Calcination and sintering, Biomaterials 23 (2002) 1073–1080.
[49] S. Raynaud, E. Champion, J.P. Lafon, D. Bernache-Assollant, Calcium phosphate apatites with variable Ca/P atomic ratio III. Mechanical properties and degradation in solution of hot pressed ceramics, Biomaterials 23 (2002) 1081–1089.
[50] H. Liu, H. Yazici, C. Ergun, T.J. Webster, H. Bermek, An in vitro evaluation of the Ca/P ratio for the cytocompatibility of nano-to-micron particulate calcium phosphates for bone regeneration, Acta Biomaterialia 4 (2008) 1472–1479.
[51] S. Raynaud, E. Champion, D. Bernache-Assollant, J.P. Laval, Determination of calcium/phosphate atomic ratio of calcium phosphate apatites using X-ray diffractometry, Journal of the American Ceramic Society 84 (2001) (2001) 359–366.
[52] B.D. Cullity, S.R. Stock, Elements of X-ray Diffraction, third ed., Prentice Hall, Inc., 2001, pp. 167–170.
[53] S.K. Pratihar, M. Garg, S. Mehra, S. Bhattacharyya, Phase evolution and sintering kinetics of hydroxyapatite synthesized by solution combustion technique, Journal of Materials Science: Materials in Medicine 17 (2006) 501–507.
[54] T. Tian, D. Jiang, J. Zhang, Q. Lin, Synthesis of Si-substituted hydroxyapatite by a wet mechanochemical method, Materials Science and Engineering C 28 (2008) 57–63.
[55] C. Kothapalli, M. Wei, A. Vasiliev, Influence of temperature and concentration on the sintering behavior and mechanical properties of hydroxyapatite, Acta Materialia 52 (2004) 5655–5663.
[56] M. Mazaheri, M. Haghighatzadeh, A.M. Zahedi, S.K. Sadrnezhaad, Effect of a novel sintering process on mechanical properties of hydroxyapatite ceramics, Journal of Alloys and Compounds 471 (2008) 180–184.
[57] J. Brandt, S. Henning, G. Michler, W. Hein, A. Bernstein, M. Schulz, Nanocrystalline hydroxyapatite for bone repair: an animal study, Journal of Materials Science: Materials in Medicine 21 (2010) 283–294.
[58] M. Pretto, A.L. Costa, E. Landi, A. Tampieri, C. Galassi, Dispersing behavior of hydroxyapatite powders produced by wet-chemical synthesis, Journal of the American Ceramic Society 86 (2003) 1534–1539.
[59] P.N. Kumta, C. Sfeir, D.H. Lee, D. Olton, D. Choi, Nanostructured calcium phosphates for biomedical applications: novel synthesis and characterization, Acta Biomaterialia 1 (2005) 65–83.
[60] P. Layrolle, A. Ito, T. Tateishi, Sol–gel synthesis of amorphous calcium phosphate and sintering into microporous hydroxyapatite bioceramics, Journal of the American Ceramic Society 81 (1998) 1421–1428.
[61] L.B. Kong, J. Ma, F. Boey, Nanosized hydroxyapatite powders derived from coprecipitation process, Journal of Materials Science 37 (2002) 1131–1134.
[62] S. Ramesh, C.Y. Tan, I. Sopyan, M. Hamdi, W.D. Teng, Consolidation of nanocrystalline hydroxyapatite powder, Science and Technology of Advanced Materials 8 (2007) 124–130.
[63] G. Georgiou, J.C. Knowles, J.E. Barralet, Dynamic shrinkage behaviour of hydroxyapatite and glass-reinforced hydroxyapatite, Journal of Materials Science 39 (2004) 2205–2208.
[64] Y.M. Sung, J.C. Lee, J.W. Yang, Crystallization and sintering characteristics of chemically precipitated hydroxyapatite nanopowder, Journal of Crystal Growth 262 (2004) 467–472.
[65] N. Patel, I.R. Gibson, S. Ke, S.M. Best, W. Bonfield, Calcining influence on the powder properties of hydroxyapatite, Journal of Materials Science: Materials in Medicine 12 (2001) 181–188.
[66] J.L. Xu, K.A. Khor, R. Kumar, Physicochemical differences after densifying radio frequency plasma sprayed hydroxyapatite powders using spark plasma and conventional sintering techniques, Materials Science and Engineering: A 457 (2007) 24–32.
[67] S. Best, W. Bonfield, Processing behaviour of hydroxyapatite powders with contrasting morphology, Journal of Materials Science: Materials in Medicine 5 (1994) 516–521.
[68] M.G.S. Murray, J. Wang, C.B. Ponton, P.M. Marquis, An improvement in processing of hydroxyapatite, Journal of Materials Science 30 (1995) 3061–3074.
[69] D.J. Curran, T.J. Fleming, M.R. Towler, S. Hampshire, Mechanical parameters of strontium doped hydroxyapatite sintered using microwave and conventional methods, Journal of the Mechanical Behavior of Biomedical Materials 4 (2011) 2063–2073.
[70] Dj. Veljovic, B. Jokic, R. Petrovic, E. Palcevskis, A. Dindune, I.N. Mihailescu, Dj. Janackovic, Processing of dense nanostructured HAP ceramics by sintering and hot pressing, Ceramics International 35 (2008) 1345–1351.
[71] N. Thangamani, K. Chinnakali, F.D. Gnanam, The effect of powder processing on densification, microstructure and mechanical properties of hydroxyapatite, Ceramics International 28 (2002) 355–362.
[72] S. Ramesh, C.Y. Tan, S.B. Bhaduri, W.D. Teng, I. Sopyan, Densification behaviour of nanocrystalline hydroxyapatite bioceramics, Journal of Materials Processing Technology 206 (2008) 221–230.
[73] O. Prokopiev, I. Sevostianov, Dependence of the mechanical properties of sintered hydroxyapatite on the sintering temperature, Materials Science and Engineering: A 431 (2006) 218–227.
[74] T.P. Hoepfner, E.D. Case, The influence of the microstructure on the hardness of. sintered hydroxyapatite, Ceramics International 29 (2003) 699–706.
[75] S. Li, H. Izui, M. kano, T. Watanabe, The effects of sintering temperature and pressure on the sintering behaviour of hydroxyapatite powder prepared by spark plasma sintering, Journal of Biomechanical Science and Engineering 3 (2008) 1–12.